27th EPS Conference on Contr. Fusion and Plasma Phys. Budapest, 12-16 June 2000 ECA Vol. **24B** *(2000) 1613 -1616*

ICRF Fast Wave and Mode Conversion Current Drive Scenarios on ASDEX Upgrade

F. Meo, M. Brambilla, J-M. Noterdaeme, D. Hartmann, G. Pereverzev, O. Gruber, and the ASDEX Upgrade team

Max-Planck-Institut für Plasmaphysik, EURATOM Association, D-85748 Garching, Germany

Introduction: In addition to supplying non-inductive current to tokamaks, Ion Cyclotron Current Drive (ICCD) can also play a key role in modifying the current profile to improve confinement. For different ICRF schemes the power absorption, the current drive efficiency, the launched k spectrum, and the radial location of the driven current must be optimised. This paper presents a summary of simulations of two ICCD scenarios for the present set-up of the ICRF system on ASDEX-Upgrade: Fast Wave (FW) for on-axis current drive (FWCD) in a deuterium plasma, and mode converted Ion Bernstein wave (^{3}He in D) for off-axis current drive (MCCD). Preliminary experimental results will also be presented.

ICRF System at ASDEX Upgrade: The ICRF system at ASDEX Upgrade (R = 1.65 m, a = 0.5 m) has four generators, each capable of delivering 2 MW of power via coaxial feeding lines to four double strap antennas [1]. The system has been recently upgraded with cross-over feeding lines providing 90^o phasing between straps necessary for current drive. The system can operate in different frequencies from 30-120 MHz. Presently, current drive has been set up at 30MHz. The symmetric power spectrum (heating case) peaks at n_ϕ = 12 while the asymmetric power spectrum (current drive case) peaks at n_ϕ = 6, where $n_\phi = k_\parallel R = R\,\omega\, n_\parallel c^{-1}$). The directionality of the asymmetric power spectrum at 30 MHz is about 60%.

Simulation tools: Two 3D finite element full wave codes are used to help understand and guide through the physics of ICCD. Both codes solve the finite Larmor radius (FLR) equations in the ion cyclotron frequency range. They describe the compressional and shear Alfven waves and the lowest ion Bernstein (IB) waves excited by mode conversion. Both include electron Landau damping of IB Waves. FELICE is a full wave code in a slab geometry. The code solves the wave equations over a n_ϕ spectrum in either the whole plasma with a metallic boundary or with an outward radiation condition at some point in the plasma. The latter procedure helps to investigate single pass absorption. FELICE also contains a self-consistent antenna evaluation section which can calculate (in simple geometry) the power spectra and antenna loading resistance. TORIC [2] solves the FLR equations in an arbitrary toroidal geometry at one n_ϕ. TORIC has been upgraded to include current drive efficiency from the Ehst-Karney parameterisation [3] for the $k_\parallel$ calculated by TORIC.

On-axis Fast Wave Current Drive (FWCD): The compressional Fast Waves (FW) are absorbed directly by the electrons through a combination of ELD and Transient Time magnetic pumping. FWCD has already been demonstrated on DIII-D [4]. The total current drive will depend on the current drive efficiency and the absorption. The single pass FW absorption $\propto \omega\, n^{3/2}\, T_e\, B^{-3}$ for $v_{phase} \sim v_{thermal}$ and the largest absorption will occur at $v_{phase} / v_{thermal} \sim 0.7$ [4], favouring large n_ϕ. The CD efficiency, on the other hand, scales as T/n, favouring smaller n_ϕ. The antenna spectrum can be chosen to deposit power in the desired portion of the particle distribution function. For the ICCD on ASDEX, $v_{phase} / v_{thermal} \sim 1$ for n_ϕ = 12 at T = 3keV. Even under the best conditions, however, the single pass absorption for the FW is weak (< 15%), making this scenario susceptible to parasitic effects in the edge. The scenario chosen for *f* = 30 MHz is one where there are no resonance layers in the main part of the plasma. At B_T = 2.9 T and low minority hydrogen concentration ([H] = H/n_e < 5%), the ion-ion hybrid layer should be about 15 cm behind the antenna and the fundamental resonance of D on the high field side just inside the scrape off layer. Above a minority concentration ≈ 20%, the mode conversion layer enters the scrape off layer. Figure 1(a) shows the antenna spectrum (90^o phasing in an ideal case) for the ICRF Antenna. Figures 1(b) and 1(c) show the current drive efficiency for minority concentrations of 5% and 20% respectively calculated by a series of TORIC runs at every n_ϕ. The parameter used were T(0) = 6 keV, $n_e(0) = 6\times10^{19}$ m^{-3} Ip = 0.8 MA. Comparing figures 1(b) and 1(c), CD efficiency is larger (peaked at n_ϕ = 5) for the low [H] whereas a larger concentration will reduce the efficiency at these lower n_ϕ values. The reason for this lies with the increased excitation of IB waves for n_ϕ < 10 for [H] = 20% case, which reduces the power in the FW. According to the Ehst-Karney parameterisation [3], electrostatic waves (IB Waves) are less efficient in driving current than electromagnetic waves (FW). In addition, IB waves absorption occurs in the thermal region where the efficiency is lowest. Therefore, with a lower n_ϕ spectrum, the FW will have a better current drive efficiency, but the minority concentration must be well controlled to minimize mode conversion. Figure 2 shows the predicted total current density at [H] = 5% weighted over the whole n_ϕ spectrum (shown in Fig. 1 (a)) at three different central temperatures. The peak current density increases linearly with central temperature. The current density for the [H] = 20% is about 30-50% lower. Excitation of IB waves due to edge gradients has been extensively studied and do not affect the overall power balance unless the decay length is smaller that 2 cm. Preliminary experiments have shown a significant difference between CD and heating. The CD induces enhanced edge effects preventing effective central absorption. In addition, unlike the heating case, the total radiation (P_{rad}) from the plasma increases monotonically during CD. One possible explanation to this increasing P_{rad} is the use of silicon to condition the vessel walls during this campaign instead of Boron. Silicon has a self sputtering coefficient > 1 whereas Boron has self sputtering coefficient < 1. There have been cases where the electron cyclotron emission (ECE) measures a significant increase in the local temperature in the vicinity of the separatrix. This local increased signal is most probably caused by fast electrons.

Off-axis Mode Conversion Current Drive (MCCD): The scenario of interest has B_T = 2,8 – 2.9 T and [^{3}He] ≈ 10-20 %, which places the He resonance at r/a = 0.2 and the mode conversion layer about mid radius on the high field side, to minimise the effect of trapped particles. In this scenario, the single pass absorption of the IB waves is appreciably higher than in the FW case. Power to the minority helium ions in single pass absorption is about 5% at T = 3keV and increases slightly with temperature. The power absorption to the IB waves decreases with temperature, but at the same time the CD efficiency should increase linearly with temperature. Therefore, it is important to calculate the total current density over the whole CD n_ϕ spectrum. Figure 3 shows the current drive efficiency as a function n_ϕ, for B_T=2.9 T, [He] = 15%, [H] = 5%, $n_e(0) = 6\times10^{19}$ m^{-3}. The current drive efficiency is peaked at n_ϕ ≈ 3. Analysing the power balance to the electrons has shown that for n_ϕ < 10, more that 90% of the power to the electrons are coupled via the IB waves. Calculated current density over the CD spectrum shows a narrow profile located at r/a = 0.45 and peaking at 300 kA m^{-2}/MW_{inc} for a total current of 15 kA/MW_{inc}. The calculated current density also revealed that there is no significant dependence of the MCCD on the central temperature at least for the range of 3-9 keV. It is important to note that these calculations do not take into account modification of the k spectrum due to refraction [6]; therefore, this is most likely an overestimation. On the other hand, insufficient numerical resolution in the code may also overestimate the coupling power to the minority ions. The preliminary MCCD experiments were performed in L-mode with ^{3}He constant puffing with Te(0) = 3 keV and n_e-bar = 6-8 $\times 10^{19}$ m^{-3}, B_T = 2.8, Ip = 0.8 MA, 5.2 MW neutral beam, and 2.2 MW ICCD (co- or counter-CD). To determine the position of the mode conversion, we also performed modulation of 50% of full power at 62.5 Hz. Figure 4 shows the ECE modulation amplitude at the ICRF modulation frequency as a function of ρ_{pol} at two different times during the discharge for both co and counter current drive. We see clearly that the deposition of power in the early part of the discharge (solid symbols) is located at ρ_{pol} = 0.65 and moves inward to ρ_{pol} = 0.55 in the later part of the discharge (open symbols) for both co- and counter current drive. TORIC predicts that deposition at ρ_{pol} = 0.65 corresponds to [He]=15-20 % and ρ_{pol} = 0.55 [He] = 10-15 %. This inward movement of the deposited power indicates a reduction of the He concentration in the region where mode conversion takes place. However, during the discharge, the electron density rises despite the clsed gas valves and there is a cooling of the edge. This suggests an hollow profile of the ^{3}He concentration. The simulation assumes that the He/n_e profile is constant throughout the plasma. These experimental results highlight the added problem of ^{3}He penetration and outward transport. Simulations with the transport code Astra have shown that the influence of the current profile by an off-axis current (after resistive relaxation) will also depend on the location of the driven current. Preliminary analysis have shown that for an ASDEX Upgrade plasma current profile (B_T=2.9, I_p = 0.8 MA, T_e(0) = 3 keV, ne(0) = 6 $\times 10^{19}$ m^{-3}, $\tau_{sawteeth}$ = 50 ms), the total current profile is not affected by an additional off-axis CD at ρ = 0.45. However at $\rho > 0.45$: co (ctr)-CD flattens (peaks) the profile hence decreasing (increasing) the internal inductance. At $\rho < 0.45$: co (ctr)-CD peaks (flattens) the profile: increasing (decreasing) l_i. On the other hand, in MCCD experiments on TFTR [7] driving off-axis co-current at r/a = 0.2 flattened the current profile. In addition, the influence of MHD activity on the rigidity of the current profile should be investigated.

Conclusions and discussion: The simulation codes, FELICE and TORIC, offer a valuable tool to investigate the physics thus optimising conditions to use ICRF to heat and drive current. The power balance between the IB waves and FW will effect the n_ϕ dependence on current drive efficiency since they have different CD efficiencies. For FWCD, if IB which are strongly coupled at low n_ϕ, are minimised, the largest current drive efficiency will be at $n_\phi \approx 5$ close to the antenna spectrum peak of n_ϕ = 6. However, this comes with a price since lower n_ϕ (higher v_{ph}) will have a lower absorption per transit hence will be more susceptible to parasitic edge effects not included in the codes. Preliminary experiments have demonstrated how important central absorption is in FWCD. Therefore the most important improvement should be the single pass absorption of the FW. Improvements include increasing the applied frequency, increasing the temperature and working at lower B_T. Reducing the density would improve the current drive efficiency and reduce the parasitic effects at the edge. The edge effects during the experiments are enhanced due to the use of silicon for wall conditioning. For MCCD, there is experimental evidence of a ^{3}He concentration profile that evolves during the plasma pulse despite the strong helium puff. The addition of extra hydrogen may reduce the need to inject more ^{3}He to move the mode conversion outward. Finally, preliminary Astra analysis showed that the effect on the current profile also depends on which radial position the driven current is applied.

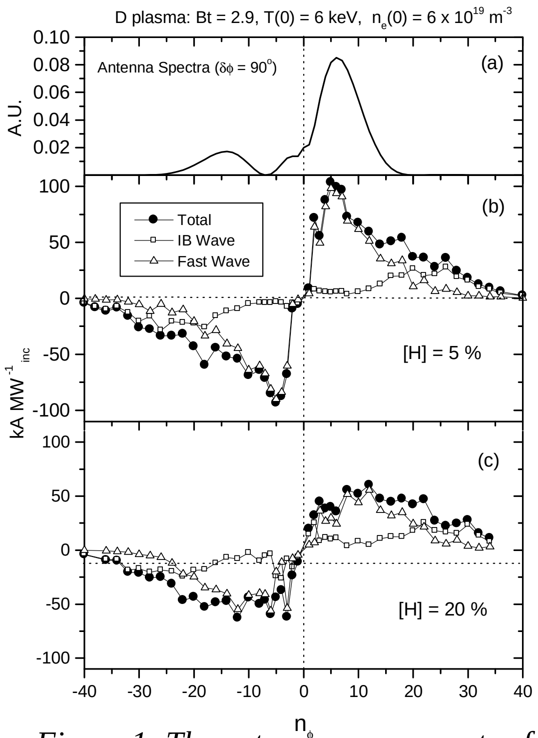

Figure 1: The antenna power spectra for the current drive (30 MHz) (b) and (c) The current drive efficiency for FWCD calculated by TORIC for [H] = 5% and 20% respectively.

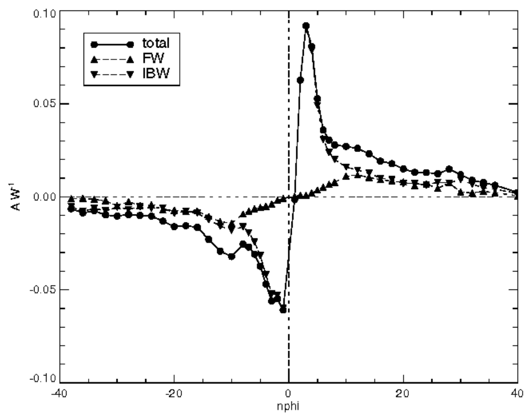

Figure 3: The current drive efficiency calculated by TORIC for mode conversion current drive (^{3}He in D)

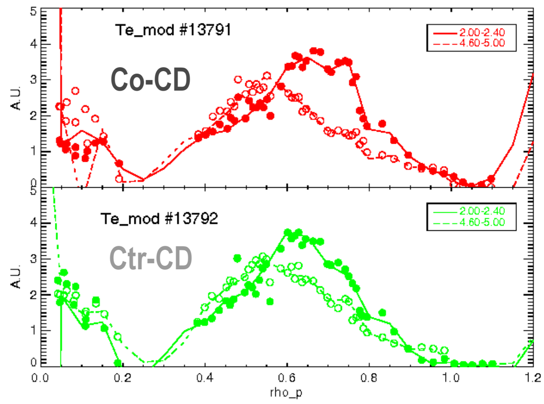

Figure 4. Modulation temperature of the ECE diagnostic during off-axis CD experiments

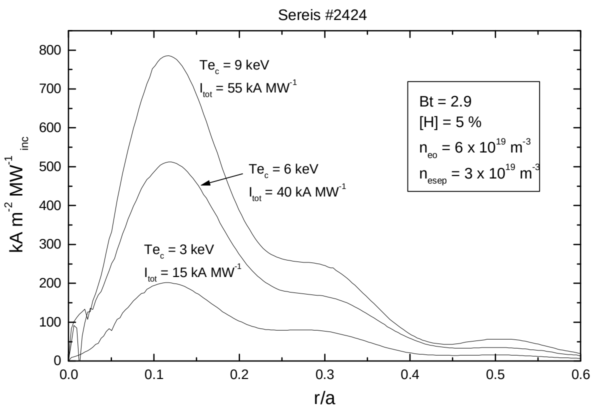

Figure 2: The calculated current density weighted over the current drive n_ϕ spectrum for the FWCD.

References:

[1] J. M. Noterdaeme, et al Fusion Engineering and Design **24** (1994) 65-74

[2] Brambilla, Plasma Phys. Controlled Fusion **41** (1999) 1

[3] D. A. Ehst and C. F. F. Karney, Nucl. Fusion **31** (1991) 1933

[4] M. Porkolab, Proceedings Stix Symposium May 4, 1992

[5] C.C. Petty, F.W. Baity, J.S. deGrassie et al, Nuclear Fusion **39** (1999) 10

[6] M. Brambilla, these proceedings

[7] R. Majeski et al., Phys. Rev. Let, **76** (1996) 5